OPEN ACCESS

University of BRISTOL

Thirunavukkarasu, T., Sparkes, H. A., & Natarajan, K. (2018). Quinoline based Pd(II) complexes: Synthesis, characterization and evaluation of DNA/protein binding, molecular docking and in vitro anticancer activity. *Inorganica Chimica Acta*, *482*, 229-239. https://doi.org/10.1016/j.ica.2018.06.003

Peer reviewed version

License (if available):
CC BY-NC-ND

Link to published version (if available):
10.1016/j.ica.2018.06.003

Link to publication record in Explore Bristol Research
PDF-document

This is the author accepted manuscript (AAM). The final published version (version of record) is available online via Elsevier at https://www.sciencedirect.com/science/article/pii/S0020169318301361 . Please refer to any applicable terms of use of the publisher.

University of Bristol - Explore Bristol Research

General rights

This document is made available in accordance with publisher policies. Please cite only the published version using the reference above. Full terms of use are available:
http://www.bristol.ac.uk/pure/about/ebr-terms

Quinoline based Pd(II) complexes: Synthesis, characterization and evaluation of DNA/protein binding, molecular docking and *in vitro* anticancer activity

Thangavel Thirunavukkarasu[a], Hazel A. Sparkes[b], Karuppannan Natarajan[c*]

[a]Department of Chemistry, CBM College, Coimbatore 641042, India

[b]Department of Chemistry, University of Bristol, Cantock's Close, Bristol, BS8 1TS, UK

[c]Department of Chemistry, Bharathiar University, Coimbatore 641046, India

*Corresponding author Email: knatraj66@gmail.com

Abstract

Two new Pd(II) complexes have been prepared from 2-methyl 4-amino quinoline and $[PdCl_2(EPh_3)_2]$ (E = P or As). The complexes, $[PdCl_2(L)(PPh_3)]$ and $[PdCl_2(L)(AsPh_3)]$ were characterized by elemental analysis, NMR, IR and UV-Vis absorption spectroscopy and single crystal X-ray diffraction. The binding affinity and the binding mode of the ligand and the complexes toward CT-DNA/BSA were determined by spectrophotometric titrations and strong interaction of the complexes with CT-DNA and BSA has been observed. An *in vitro* cytotoxicity study of the compounds against human lung (A-549) and breast (MCF-7) cancer cell lines gave IC_{50} values for both the ligand and the two complexes in the range of Cisplatin and Doxorubicin.

Keywords: Quinoline; Pd(II) complexes; DNA/protein binding; Cytotoxicity.

Introduction

Currently, one of the most important areas of research in bioinorganic chemistry is the design and synthesis of transition metal complexes as efficient anticancer agents [1–5]. In this connection, Pd(II) complexes have attracted the attention of bioinorganic chemists as potential alternative to cisplatin that is being currently administered because of the fact that the Pd(II) complexes can undergo aquation and ligand exchange reactions 10^5 times faster than the corresponding Pt(II) complexes. Hence, a new area of active research in bioinorganic chemistry has emerged recently targeting new drugs of cancer cell specific [6-8] and a number of Pd(II) complexes [9-15] have even shown better anticancer properties that that of Pt(II) complexes due to the structural and thermodynamic similarities between Pd(II) and Pt(II) complexes.

As far as the ligands used for the synthesis of new Pd(II) complexes is concerned, quinolines are best suited since they are a class of compound that has been used in agriculture as fungicide besides being used as preservatives in wood, paper and textile industries [16]. In this connection, it is to be noted that alkaloid and alkaloid based compounds contain quinoline as an

important structural unit which exhibited substantial biological activities [17,18]. Moreover, the biological activities such as antioxidation, antiproliferation and anticancer have also been exhibited by the derivatives of quinolones [19-22]. This has really created a special interest in the synthesis of transition metal complexes of quinolines and to study their role in inhibiting cancer cell proliferation and microbial growth [23-26]. The results have indicated that the complexes thus prepared have not only shown significant pharmacological properties but also revealed interesting coordination modes of quinolines in the complexes. Hence, we synthesized two new Pd(II) complexes from aquinoline derivative. Interestingly, the complexes contain the ligand coordinated through the quinoline pyridine nitrogen atom only. Herein, we report the synthesis, structures, DNA interactions, protein binding, molecular docking and cytotoxicity studies of mononuclear palladium complexes of 2-methyl 4-amino quinoline.

Results and discussion

Synthesis

The preparative route for the new complexes $[PdCl_2(L)(PPh_3)]$ and $[PdCl_2(L)(AsPh_3)]$ is shown in **Scheme 1**. The new complexes were prepared by the reaction of the 2-methyl 4-amino quinoline with $[PdCl_2(PPh_3)_2]$ or $[PdCl_2(AsPh_3)_2]$ in toluene. They were obtained in good yields and characterized by IR, UV-visible, fluorescence spectroscopy, ^1H NMR and single crystal X-ray diffraction methods. Both the ligand and complexes are air stable. They are soluble in methanol, ethanol and methylene dichloride, trichloromethane, dimethylformamide and dimethylsulfoxide.

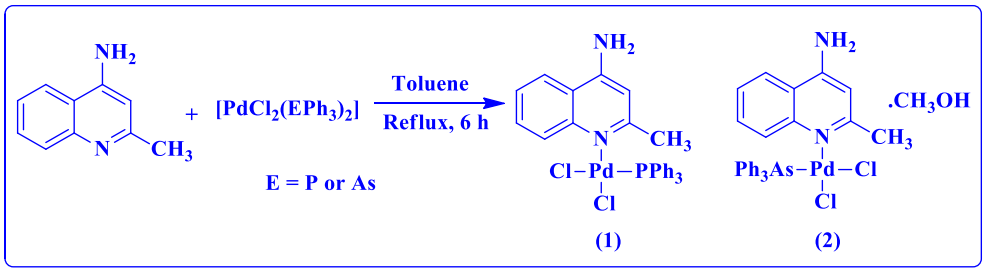

Scheme 1. Preparation route of the Pd(II) complexes.

Spectroscopy

Electronic spectra of the complexes showed two strong absorption bands, one in the regions at 260-264 corresponding to intra ligand transition and the other at 315-328 nm which has been assigned to ligand to metal charge transfer transition [27]. The IR spectra of the complexes $[PdCl_2(L)(PPh_3)]$ and $[PdCl_2(L)(AsPh_3)]$ displayed characteristic absorption bands in the regions 3373-3391 and

1356-1359cm^{-1} due to (-NH_2) and (-CH_3) vibrations respectively. The aromatic (C=N) frequency for the free ligand which appeared at 1610-1614 has been shifted to 1642-1638 cm^{-1} for the complexes 1 and 2 indicating that the palladium ion is coordinated to the nitrogen atom. The ^{1}H NMR spectra of the complexes are shown in Figures S1 & S2. The signal due to –NH_2 proton was observed as doublets at δ 8.14-8.17 and 9.48-9.50 ppm in the spectra of [$PdCl_2$(L)(PPh_3)] and [$PdCl_2$(L)($AsPh_3$)]. Two singlets appeared at δ 2.89 and 2.97 ppm for methylene protons in the complexes. Further the spectra of the two complexes showed a series of overlapping multiplets for aromatic protons at δ 7.30-7.89 and 6.73-7.43 ppm respectively.

Crystallography

Complex [$PdCl_2$(L)(PPh_3)] consists of a distorted square planer Pd(II) metal center coordinated to two cis chloride ligands, a PPh_3 group and a quinoline which was attached in a neutral manner through the pyridyl N as shown Figure1. The compound crystallized in the monoclinic space group $P2_1/c$ with two unique molecules in the asymmetric unit (Z'=2) with two molecules in the asymmetric unit. Intermolecular π-π interactions were identified between pairs of quinolone rings between one of the phenyl rings and the quinolone Table 1 and Figure2. Intermolecular N-H···Cl hydrogen bonding was also identified (Table S1).The crystal structure of complex [$PdCl_2$(L)($AsPh_3$)] was obtained as a solvate with methanol with a distorted square planar Pd(II) metal center coordinated to two cis chloride ligands, a $AsPh_3$ group and a quinoline which was attached in a neutral manner through the pyridyl N shown in Figure 3. This complex crystallized in the monoclinic space group $P2_1/n$ with one molecule of [$PdCl_2$(L)($AsPh_3$)] in the asymmetric unit along with methanol. Intermolecular hydrogen bondings O-H···Cl, N-H···O and N-H···Cl were identified but no π-π interactions were seen in this case (Table 1). The data collection and parameters of refinement progression are given in Table **3** and important bond lengths and bond angles are summarized in Table 4.

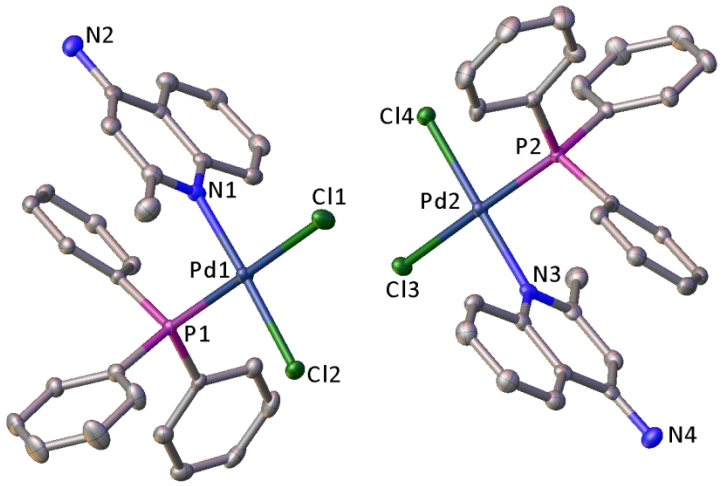

Figure 1. Molecular structure of complex **1**.

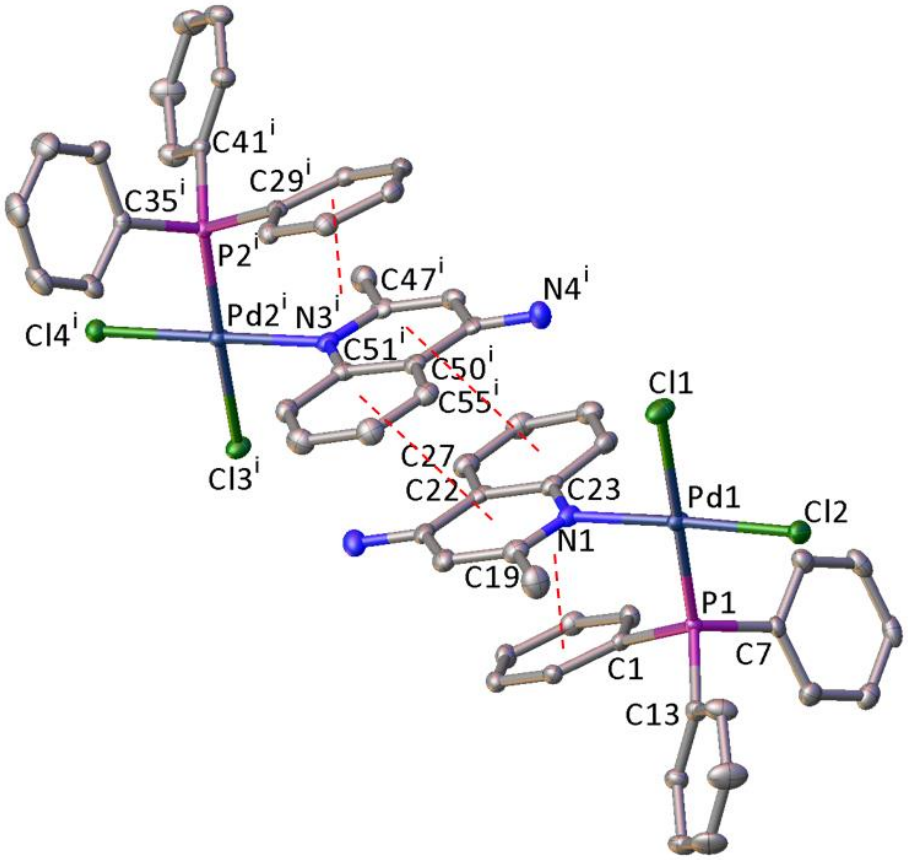

Figure 2. Molecular structure of Intermolecular π-π interactions in complex [$PdCl_2$(L)(PPh_3)]

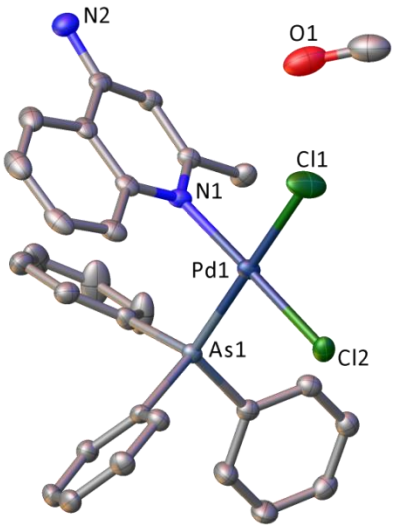

Figure 3. Molecular structure of complex $[PdCl_2(L)(AsPh_3)]$.

Table 1. π-π interactions in complex $[PdCl_2(L)(PPh_3)]$

Ring 1	Ring 2	Centroid-centroid (Å)	Shift (Å)
Complex **1**			
C1-C6	C22-C27^{i}	3.539	1.017
C1-C6	N1, C19-C23^{i}	3.416	1.556
C22-C27	N3, C47-C51^{ii}	3.619	1.487
N1, C19-C23	C50-C55^{ii}	3.686	1.746
N1, C19-C23	N3, C47-C51^{ii}	3.831	2.045
C29-C34	C50-C55^{i}	3.644	1.279
C29-C34	N3, C47-C51^{i}	3.354	1.308

i $+x, +y, +z$; ii $1+x, +y, +z$

Table 3. Crystal structure data for the complex $[PdCl_2(L)(PPh_3)]$ and $[PdCl_2(L)(AsPh_3)]$.

Identification code	$[PdCl_2(L)(PPh_3)]$	$[PdCl_2(L)(AsPh_3)]$
CCDC number	1498615	1498616
Empirical formula	$C_{28}H_{25}Cl_2N_2PPd$	$C_{28.8}H_{28.2}AsCl_2N_2O_{0.8}Pd$
Formula weight	597.77	667.35
Temperature/K	100(2)	100(2)
Crystal system	monoclinic	Monoclinic
Space group	$P2_1/c$	$P2_1/n$
a/Å	10.2603(5)	10.7382(2)
b/Å	28.1702(14)	17.4602(2)
c/Å	17.1676(8)	14.5297(2)
α/°	90	90
β/°	90.614(3)	105.2002(7)
γ/°	90	90
Volume/Å^3	4961.7(4)	2628.89(7)
Z	8	4
ρ_{calc}g/cm^3	1.600	1.686
μ/mm^{-1}	1.048	2.183
F(000)	2416.0	1338.0
Crystal size/mm^3	0.39 × 0.28 × 0.21	0.47 × 0.28 × 0.24
Radiation	MoKα (λ = 0.71073)	MoKα (λ = 0.71073)
2Θ range for data collection/°	2.778 to 55.78	3.726 to 55.906
Index ranges	$-13 \le h \le 13$, $-28 \le k \le 37$, $-22 \le l \le 22$	$-14 \le h \le 10$, $-23 \le k \le 21$, $-19 \le l \le 19$
Reflections collected	44782	23594
R_{int}	0.0389	0.0270
Data/restraints/parameters	11812/0/631	6306/13/336

Goodness-of-fit on F^2	1.081	1.048
Final R indexes [I>=2σ (I)]	R_1 = 0.0408, wR_2 = 0.0825	R_1 = 0.0270, wR_2 = 0.0608
Final R indexes [all data]	R_1 = 0.0561, wR_2 = 0.0889	R_1 = 0.0351, wR_2 = 0.0640
Largest diff. peak/hole / e $Å^{-3}$	1.27/-0.72	1.16/-0.85

Table 4. Particular bond lengths (Å) and bond angles (°) in the complexes

Bond length (Å) $[PdCl_2(L)(PPh_3)]$	**Bond length (Å)** $[PdCl_2(L)(AsPh_3)]$
Pd1-Cl1-2.3789(8)	Pd1-As1-2.3506(3)
Pd1-Cl2-2.3092(8)	Pd1-Cl2-2.2945(6)
Pd1-P1-2.2571(8)	Pd1-Cl1-2.3411(7)
Pd1-N1-2.047(3)	Pd1-N1-2.040(2)
N1-C19-1.346(4)	**Bond angle (°)**
N1-C23-1.373(4)	Cl2-Pd1-As1-88.849(17)
Bond angle (°)	Cl2-Pd1-Cl1-91.51(3)
Cl2-Pd1-Cl1-91.37(3)	Cl1-Pd1-As1-178.71(3)
P1-Pd1-Cl1-179.41(3)	N1-Pd1-As1-92.14(5)
P1-Pd1-Cl2-89.20(3)	N1-Pd1-Cl2-176.72(6)
N1-Pd1-Cl1-89.77(7)	N1-Pd1-Cl1-87.57(6)
N1-Pd1-Cl2-177.30(8)	Cl1-As1-Pd1-113.83(7)
N1-Pd1-P1-89.67(7)	C23-As1-Pd1-113.59(7)
C1-P1-Pd1-114.44(10)	C23-As1-Cl1-103.95(10)
C7-P1-Pd1-115.20(10)	C17-As1-Pd1-115.38(7)
C13-P1-Pd1-114.09(11)	C6-N1-Pd1-118.65(16)
C2-N1-Pd1-121.68(16)	

DNA binding studies

DNA binding of the ligand and the new compounds was carried out as it is considered one of the important aspects in deciding whether a compound could be an anticancer drug [28,29]. Electronic absorption titration is the effective method to test the binding modes of compounds with DNA [30]. The spectral features will be seen in terms of hyperchromism and hypochromism concerned with modifications of DAN double helix structure. The interaction of the compounds with CT-DNA was followed by recording the UV-visible spectra by the increased addition of the CT-DNA to the test compounds (Figure 4). When the ligand was titrated against CT-DNA, the absorption bands of the ligand exhibited hyperchromism with a red

shift of4 nm. In the case of the complex[$PdCl_2$(L)(PPh_3)], on the addition of DNA, it exhibited hyperchromism with a red shift of 4 nm and complex [$PdCl_2$(L)($AsPh_3$)] exhibited hyperchromism without any wavelength shift. Complex [$PdCl_2$(L)(PPh_3)] showed more hyperchromicity than that of the ligand and complex [$PdCl_2$(L)($AsPh_3$)] indicating more binding strength for the complex [$PdCl_2$(L)(PPh_3)]. From the plot of [DNA]/(ε_a-ε_f) *versus* [DNA] (Figure 5), the intrinsic binding constants K_b were calculated and they were found to be 0.342×10^6, 1.6528×10^6 and 0.5660×10^5 M^{-1} for the ligand and the complexes [$PdCl_2$(L)(PPh_3)] and [$PdCl_2$(L)($AsPh_3$)] respectively indicating that the ligand and the complexes bind to DNA *via* an intercalative mode [31].

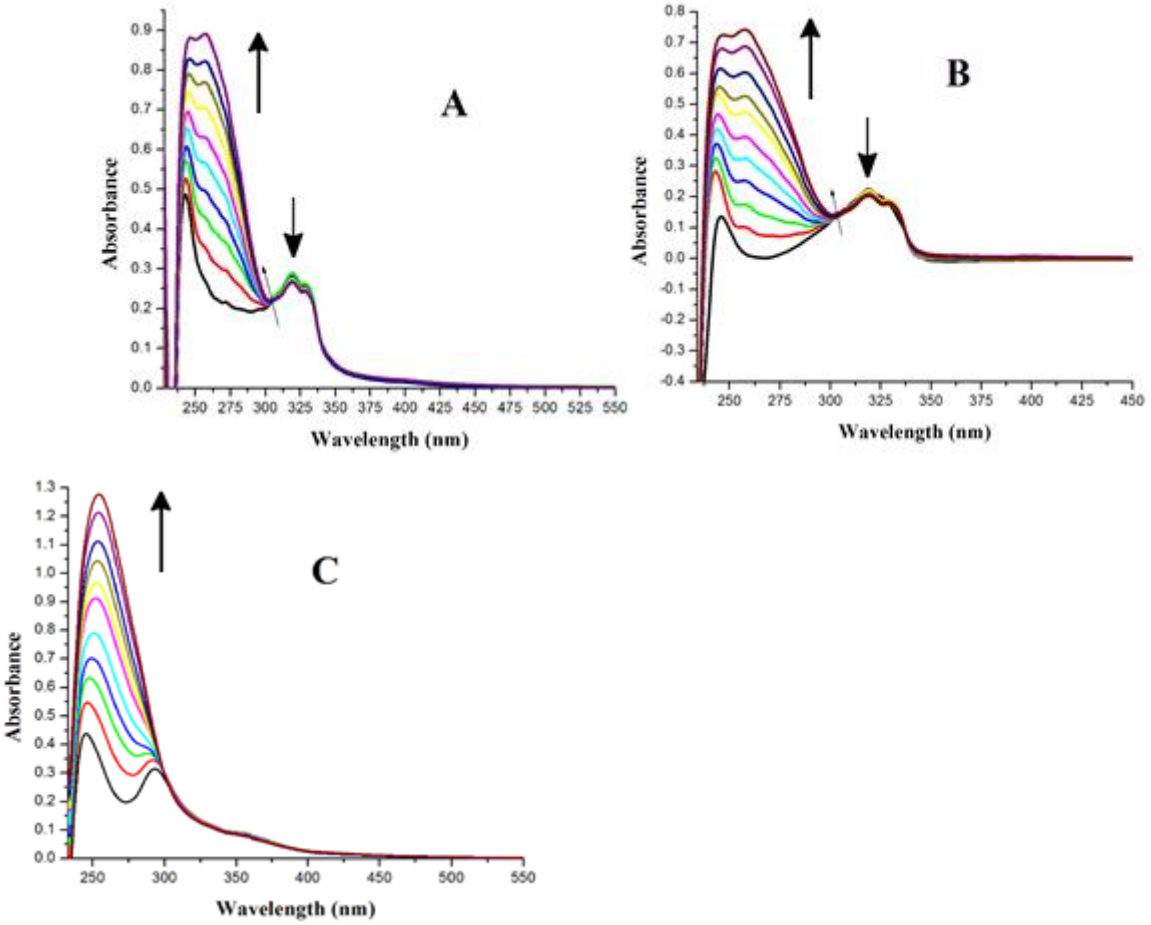

Figure 4. Absorbtion titration of the compounds in the absence and presence of CT-DNA. Ligand (A), complex[$PdCl_2$(L)(PPh_3)] (B), and complex [$PdCl_2$(L)($AsPh_3$)] (C). [Compounds] = 10 µM, [DNA] = 0-100 µM. Arrow indicatesthat the absorption intensities increase upon incremental concentration of DNA.

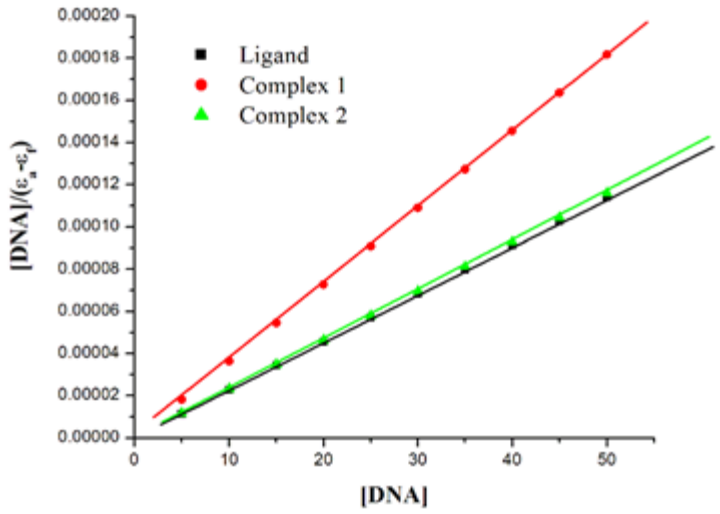

Figure 5. Plot of [DNA]/(ε_a-ε_f) *versus* [DNA].

Ethidiumbromide(EB) displacement study

Though the electronic absorption studies indicate that the compounds efficiently bind to DNA, it is not enough to conclusively say that there exists a binding and hence, there is a need to prove this by other studies. In this connection, ethidiumbromide(EB) displacement experiments are considered to be the best technique to confirm the binding mode. Since EB forms soluble compounds with nucleic acids and emits intense fluorescence in the presence of CT-DNA due to the intercalation of the planar phenanthridine ring between adjacent base pairs on the double helix [32], one can obtain information on the binding mode of any compound with DNA. In the EB displacement study, there is a decrease in the intensity of fluorescence as and when EB is displaced from a DNA sequence by a quencher and the quenching will be due to the reduction of the number of binding sites on the DNA that is available to EB. Figure S3 shows the fluorescence quenching spectra of DNA bound EB by compounds and illustrate that as the concentration of the compounds increases the emission band at 626 nm showed hypochromism. The observed decrease in the fluorescence intensity indicates that the EB molecules have been displaced from their DNA binding sites and are replaced by the test compounds [33,34]. The quenching constants and binding constants can be analyzed through a couple of equations. The following Stern-Volmer equation is used obtain the quenching constant,

$$I_0/I = K_q[Q] + 1$$

Where I_0 and I represent the emission intensities in the absence and presence of the complexes, respectively, K_q is the quenching constant, and [Q] is the concentration ratio of the complex.

From the slope of the plot of I_0/I *versus* [Q], one can obtain *K*q values (Figure S4) and the values obtained for the ligand and complexes were found to be 2.61×10^3, 4.16×10^3 and3.53×10^3 M^{-1}. These values do indicate that the ligand and Pd(II) complexes interact with DNA through intercalation mode of binding [35].

Protein binding studies

In order to find out the interaction of the compounds with protein, we undertook the study of interaction of our compounds with BSA. A constant concentration of BSA (1 µM) was titrated with various concentrations of the compounds (0–100 µM) and the fluorescence emission spectra were recorded (Figure S5). It can be seen that the effect of compounds on BSA resulted in a significant decrease in the fluorescence intensity at 347 nm with no shift in their emission wavelength maxima. The observed decrease in the fluorescence intensity could be attributed to the fact that the active site in the protein is buried in a hydrophobic environment [36,37]. By using the following Scatchard equation, the fluorescence quenching data can be analyzed.

$$\log[F_0\text{-}F/F\ ] = \log K_{bin} + n \log[\ Q]$$

Where K_{bin} is the binding constant of the compound with BSA and n is the number of binding sites. The binding constants K_{bin} have been calculated from the plot of $\log[F_0\text{-}F/F\ ]$ *versus* log[Q] as shown in (Figure S6-A). Further, from the Stern-Volmer the plot of I_0/I *versus* [Q], the quenching constants *K*q have been calculated (Figure S6-B). The values of K_q, K_{bin}, and *n*, the number of binding site are given in table 5 and the value of *n* around 1 for the ligand and complexes indicates the existence of just a single binding site in BSA with the compounds. It is to be noted here that the complex $[PdCl_2(L)(PPh_3)]$ has better binding affinity than that of the ligand and complex $[PdCl_2(L)(AsPh_3)]$.

Table 5. Quenching constant (K_q), binding constant (K_{bin}), and number of binding sites (*n*) for the interactions of compounds with BSA.

Compound	K_q (M^{-1})	K_{bin}(M^{-1})	*n*
Ligand	3.02×10^3	5.43×10^2	0.81
$[PdCl_2(L)(PPh_3)]$	9.60×10^2	4.08×10^4	0.93
$[PdCl_2(L)(AsPh_3)]$	3.88×10^3	2.77×10^2	0.76

UV absorption spectra of BSA in the presence of compounds

After having found out binding constants and the quenching constants for the compounds under study, it is necessary to know about type of quenching in order to get more insight which can be

obtained through absorption spectroscopy. Quenching usually occurs through two proesses namely, dynamic or static quenching. If the fluorophore and the quencher come into contact during the transient existence of the excited state, it is referred to asdynamic quenching and if the same takes place in ground state then it is referred tostatic quenching. The UV absorption spectra of BSA taken in the presence and absence of the compounds under study are shown in Figure 10. The absorption intensity has increased on the addition of the compounds which indicates a static quenching of the compounds with BSA [38].

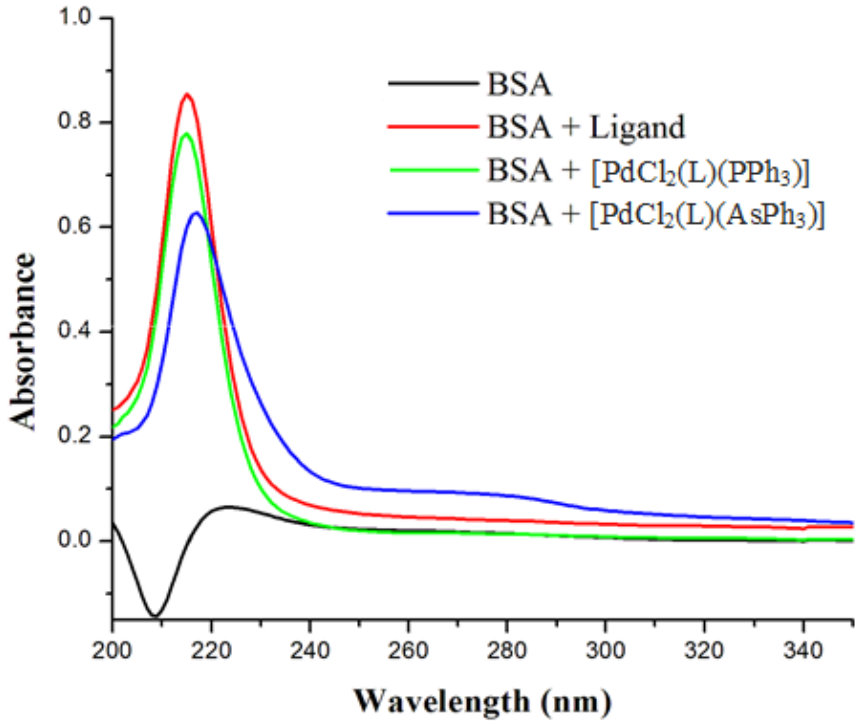

Figure 10. Absorbance titration of BSA with the ligand and complexes.

Synchronous fluorescence spectra

In addition to the studies conducted as above, synchronous fluorescence spectral studies have also been employed to observe the structural changes occurred to BSA upon the addition of compounds, particularly in the vicinity of the fluorophore functional groups [39]. It is known that fluorescence of BSA is due to the presence of tyrosine, tryptophan and phenylalanine residues and hence, fluorescence spectroscopic methods can be effectively used to study the conformation of serum protein. In this connection, it has been shown that the difference between the excitation wave length and emission wavelength ($\Delta\lambda = \lambda_{em} - \lambda_{ex}$) will indicate the type of chromophores.

Usually a $\Delta\lambda$ = 15 nm in the synchronous fluorescence of BSA is indicative of a tyrosine residue, whereas a larger $\Delta\lambda$ = 60 nm is characteristic of tryptophan. Figure 11 shows the synchronous fluorescence spectra of BSA with various concentrations of test compounds recorded at $\Delta\lambda$ = 60 nm. In the synchronous fluorescence spectra of BSA at $\Delta\lambda$ = 60, the addition of the compounds to the solution of BSA resulted in a decrease of the fluorescence intensity of BSA at 348 nm for the ligand and the complexes indicating that the tryptophan residues were affected by increasing the concentration of compounds. The result of the BSA protein binding experiments with our compounds has already revealed that the binding of the compounds with BSA is mainly hydrophobic in nature. Moreover, the binding strength of the Pd(II) complexes with BSA is significantly higher than that of the ligand, which can be explained by the fact that the hydrophobicity of the complex is greater than that of the ligand. So, the strong interaction between the Pd(II) complexes and BSA suggested that this compound can easily be stored in protein and can be released at desired target areas. Hence, it will be interesting to study the pharmacological properties of Pd(II) complexes.

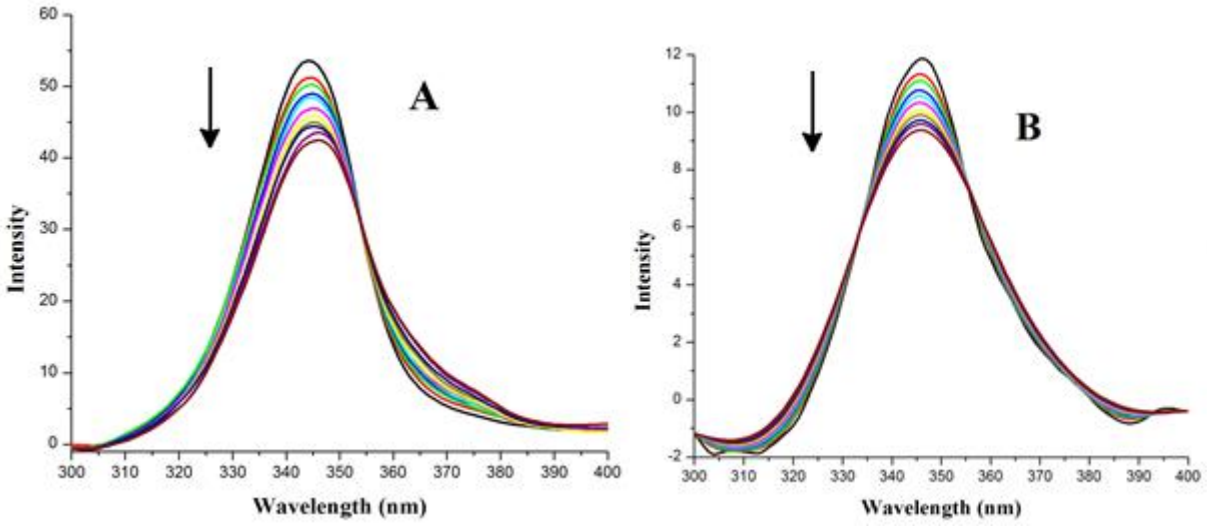

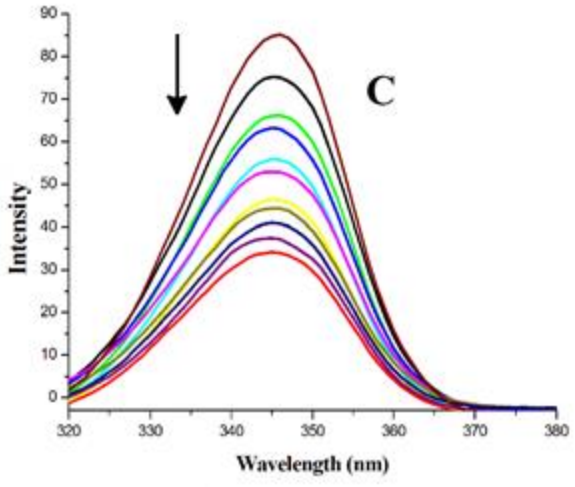

Figure 11. Synchronous spectra of BSA (1µM) in the the ligand (A), complex $[PdCl_2(L)(PPh_3)]$ (B), and complex $[PdCl_2(L)(AsPh_3)]$ (C) (0 – 100 µM) at a wavelength difference of $\Delta\lambda = 60$ nm.

Molecular docking studies

Molecular docking studies have played a very significant role in delivering a visual representation of the binding of the drugs to BSA, which can substantiate the spectroscopic results. To ascertain the binding mode of the ligands and complexes with most probable site of the bovine serum albumin (BSA), molecular docking studies have been carried out. The protein binding interaction model shown in Figure 12 and relative binding energy of the docked compounds are showed in Table 6. It has been found that the prime region for interaction of BSA with the compounds is in hydrophobic environment of the tryptophan residue. The hydrophobicity observed in the molecular docking studies confirmed the effective interaction of all the compounds with BSA in static interaction. For the ligand, the atomic interaction is between HZ1 of the protein residue LYS431 with H-atom of the quinoline aromatic ring. For the complex $[PdCl_2(L)(PPh_3)]$, the atomic interaction is between oxygen of the protein residue LEU112 with the hydrogen atom of the amine. In complex $[PdCl_2(L)(AsPh_3)]$, the atomic interaction is between OE2 of the protein residue GLU125 with the hydrogen atom of the amine. The results obtained from molecular docking studies revealed that the interaction between complex **1** and BSA is with the highest binding energy dominated by hydrophobic forces.

Table 5. Binding energy of the docked compounds.

Compounds	**Binding_energy (Kcal/mol)**	**Compound Efficiency (Kcal/mol)**	**Hydrogen bond formed**	**Hydrogen bond residues**	**Distance between residues (Aº)**
Ligand	-2.57	-0.17	1	LYS431	LYS431(2.6)
$[PdCl_2(L)(PPh_3)]$	-3.8	-0.09	1	LEU112	LEU112(2.2)
$[PdCl_2(L)(AsPh_3)]$	-3.5	-0.16	1	GLU125	GLU125(1.8)

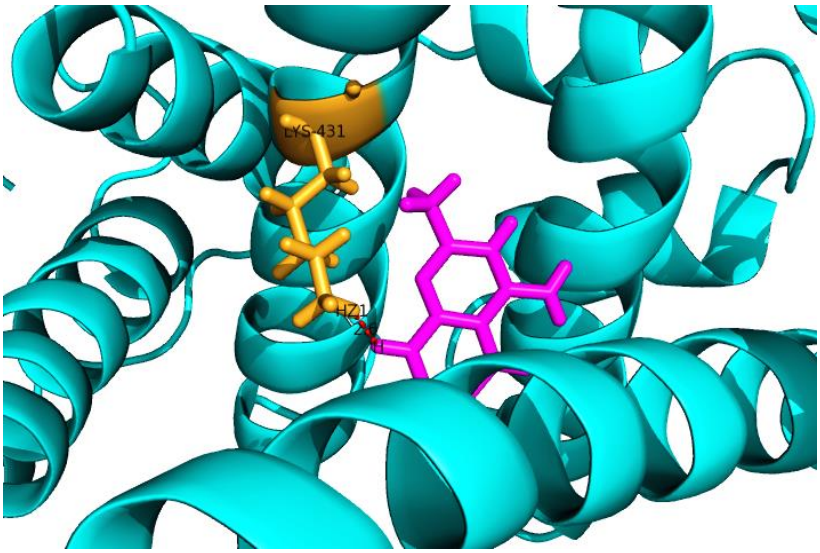

Ligand

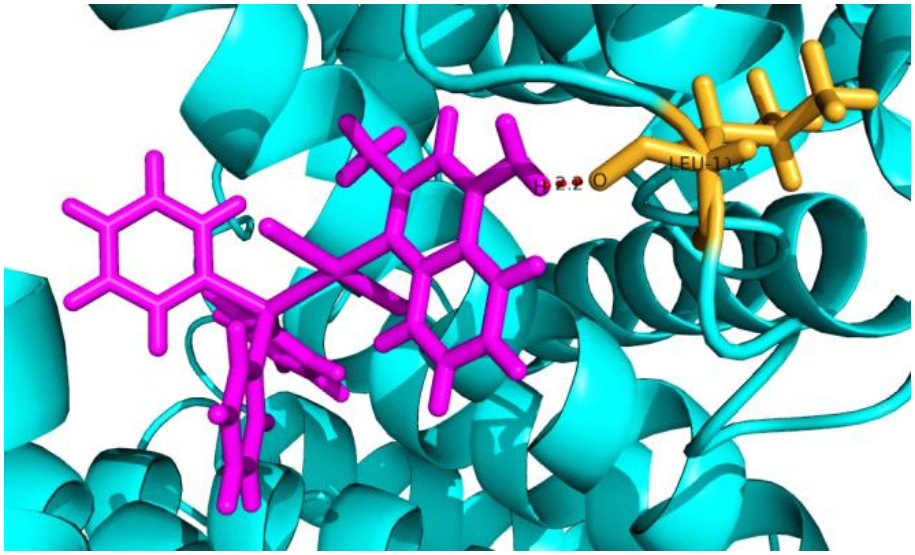

Complex [$PdCl_2(L)(PPh_3)$]

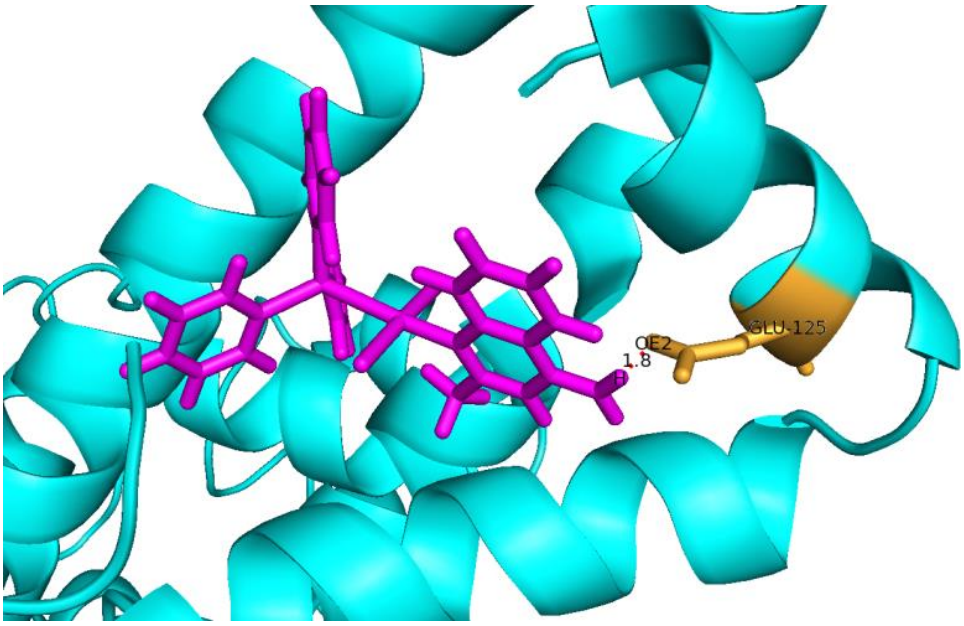

Complex [$PdCl_2(L)(AsPh_3)$]

Figure 12. Molecular docked model of the compounds.The receptor interactions with compounds was represented by magenta and protein residues are cyan and bright orange respectively.

***In vitro* cytotoxic activity evaluation**

The positive results obtained from the biological studies, namely, DNA binding, BSA binding, and BSA docking studies for our compounds prompted us to test their cytotoxicity against a panel of human lung cancer (A-549) and breast cancer (MCF-7) cell lines. *Doxorubicin* and *cisplatin* were used as a positive control to assess the cytotoxicity of the test compounds. The compounds were analyzed by means of cell inhibition expressed as IC_{50} values and bar chart which are shown in Table 7 and in Figure 13. The ligand and the complexes have shown better cytotoxic effects on the selected cancer cell lines with lower IC_{50} values specifying their efficiency in killing the cancer cells even at low concentrations. From the results obtained it has been found that the palladium complexes $[PdCl_2(L)(PPh_3)]$ and $[PdCl_2(L)(AsPh_3)]$ and the ligand produce inhibition of cell growth even at < 100 μg of concentration on cancer cells indicating that our compounds showed significant activity compared to standard anticancer drugs. From the two cell lines chosen to examine, complex $[PdCl_2(L)(PPh_3)]$ showed better cytotoxic specificity to human breast cancer cell (MCF-7) than other one. On the other hand, there is no substantial difference in the cytotoxic activities when triphenyl phosphine was replaced by triphenyl arsine in the complexes. The morphological changes examined by staining method suggested that the cell death mechanism was through apoptosis. Overall, the cytotoxicity of the complexes is very similar to that of the DNA and protein binding activity, showing a higher potential for complex$[PdCl_2(L)(PPh_3)]$ [40].

Table 7. The IC_{50} values of the compounds.

IC_{50} values (μM)		
Compound	A-549	MCF-7
Ligand	29 ± 1.1	35 ± 1.5
$[PdCl_2(L)(PPh_3)]$	30 ± 0.9	26 ± 1.4
$[PdCl_2(L)(AsPh_3)]$	31 ± 1.3	29 ± 0.7
Doxorubicin	15 ± 1.2	16 ± 1.3
Cisplatin	25 ± 2.1	18.7 ± 0.1

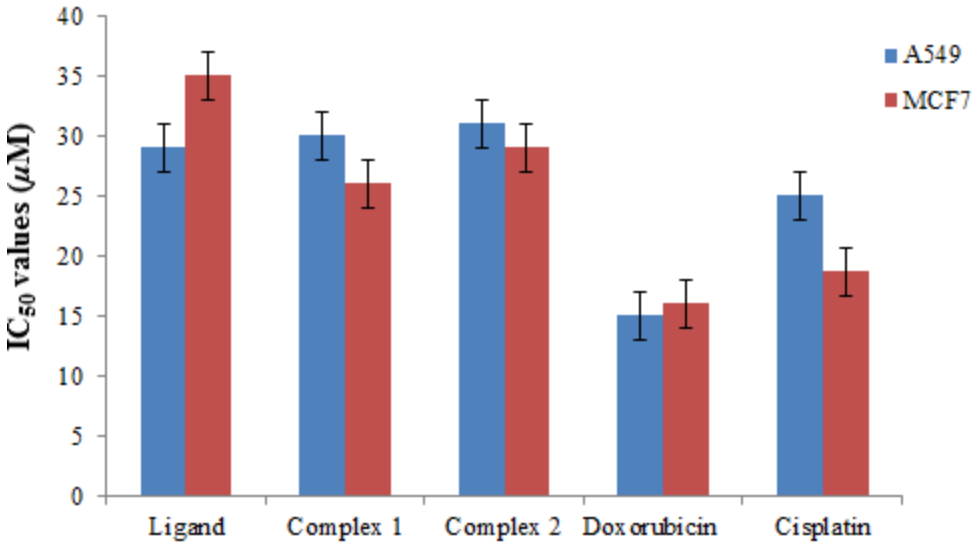

Figure 13. The IC_{50} values of compounds are depicted against (A-549) and (MCF-7) cancer cell lines.

Acridine orange /Ethidium bromide (AO/EtBr) staining method

Fluorescence microscopy images of (A-549)-(A) and (MCF-7)-(B) cancer cells in the absence of compounds (control) and in the presence of the test compounds are shown in (Figure S7). The untreated (A-549) and (MCF-7) cancer cells (control-(a), (b), (c)) did not show any significant adverse effect compared to the compounds treated with cancer cells (Figure 14-(d), (e), (f)). It can be seen that with the addition of compounds to the cancer cells, the green colour of cells are converted into orange/red colour cells which is due to induced apoptosis and the nuclear condensation effect on the cells. This indicates that the compounds were significantly inducing the apoptosis in selected cancer cells.

DAPI staining method

Further, to confirm the nuclear condensation and fragmentation of compounds on selected cancer cells, we evaluated the DAPI staining method. Fluorescence microscopy images of Lung and breast cancer cells after 24 h stained with DAPI in the absence and presence of compounds are shown in (Figure S8). It is seen from the figure that the untreated cells (a, b, c) didn't show any significant change whereas compounds treated cancer cells (d, e, f) showed bright fetches which suggest that the condensed chromatins and nuclear fragmentations in the cancer cells. Moreover, the bright patches observed for A-549and MCF-7 cell lines are higher for that are treated with the test compounds when compared that with untreated ones. Thus, from the results all the

studies carried out,we confidently report here that the compounds can be used as potent therapeutic agents.

Conclusion

The synthesis and characterization of square planar Pd(II) complexes are described. The synthesized compounds are characterized by various spectroscopic techniques. The structures of the complexes have been confirmed by single crystal X-ray diffraction studies. The coordination mode of quinoline observed in $[PdCl_2(L)(PPh_3)]$ and $[PdCl_2(L)(AsPh_3)]$ is an extremely rare case as far as the monodentate coordination behavior of quinoline is concerned. The interaction of ligand and complexes with calf thymus CT-DNA, EB displacement and bovine serum albumin (BSA) protein was investigated using absorption and fluorescence spectroscopic methods. Absorption and emission titration studies revealed that complex **1** interacts with CT-DNA through intercalative binding mode and interact to BSA with static quenching mechanism. *In vitro* cytotoxicity results showed that the complex **1** exhibited significant activity against (MCF-7) cancer cell line. The morphological changes examined by staining method suggested that the cell death mechanism was through apoptosis. By changing the substituents on the ligands, the anticancer properties of the resulting complexes may be enhanced, and it possible to design efficient multifunctional biomolecules in future.

EXPERIMENTAL SECTION

Materials and methods.

All the chemicals were purchased from sigma Aldrich and used as received. Solvents were purified and dried according to standard procedures [41]. $[PdCl_2(PPh_3)_2]$ and $[PdCl_2(AsPh_3)_2]$ were prepared by literature methods [42-44]. Elemental analyses (CHNS) were performed on Vario EL III Elemental analyzer. IR spectra (400-4000 cm^{-1}) were recorded on a JASCO FT-IR 4100 spectrophotometer with KBr discs. Melting points of the compounds were determined with a lab India instrument. The electronic spectra of the compounds were recorded with a Jasco V-630 spectrophotometer. Emission spectra were measured with Jasco FP 6600 spectrofluorometer. DNA binding, Ethidiumbromide(EB) displacement study**,** protein binding, protein docking and cytotoxicity experiments were conducted as per the reported procedures [45-49, 35].

Synthesis of the complex, $[PdCl_2(L)(PPh_3)]$**:**

To a solution of $[PdCl_2(PPh_3)_2]$ (0.100g, 0.1424 mmol) in toluene (20 cm^3), 2-methyl 4-amino quinoline, (0.022g, 0.1424 mmol) was added. The mixture was heated under reflux for 6 h during

which period a reddish brown precipitate was formed. The reaction mixture was then cooled to room temperature, and the solid compound was filtered off. It was washed with petroleum ether (60-80 ºC) and dried under *vacuum*. The complex was then recrystallized from methanol/DMF. Reddish brown crystals suitable for X-ray diffraction were obtained. Yield: 78 %. M.p.: 161 ºC. Elemental analysis calculated for $C_{28}H_{25}Cl_2N_2PPd$ (%): Cal: C, 56.26; H, 4.22; N, 4.69. Found (%): C, 56.21; H, 4.20; N, 4.62. FT-IR (cm^{-1}) with KBr disk: 3373 (υ_{NH2}), 1642 ($\upsilon_{C=N}$), 1356 (υ_{CH3}): UV-visible (Solvent DMSO, nm): 260 (Intra-ligand transition), 328 (Ligand to metal charge transfer transition).^{1}H NMR (400 MHz, DMSO-d_6, δ, ppm): δ 8.14-8.17 (d, J = 12 Hz, 2H, (NH_2)), δ 7.30-7.89 (m, Ar-H, 20H), δ 2.89 (s, 3H, (CH_3)).

Synthesis of the complex, $[PdCl_2(L)(AsPh_3)]$**:**

It was prepared by the same method as described for complex $[PdCl_2(L)(PPh_3)]$ using $[PdCl_2(AsPh_3)_2]$ (0.100g, 0.1266 mmol) and 2-methyl 4-amino quinoline, (0.020g, 0.1266 mmol). The complex was then recrystallized from methanol/toluene, which yielded yellow crystals suitable for X-ray diffraction. Yield: 84 %. M.p.: 156 ºC. Elemental analysis calculated for $C_{29}H_{29}AsCl_2N_2OPd$: Cal (%): C, 51.69; H, 4.34; N, 4.16. Found (%): C, 51.64; H, 4.29; N, 4.11. FT-IR (cm^{-1}) with KBr disk: 3391 (υ_{NH2}), 1638 ($\upsilon_{C=N}$), 1359 (υ_{CH3}): UV-visible (Solvent DMSO, nm): 264 (Intra-ligand transition),315 (Ligand to metal charge transfer).^{1}H NMR (500 MHz, DMSO-d_6, δ, ppm): δ 9.48-9.50 (d, J = 10 Hz, 2H, (NH_2)),δ 6.73-7.43 (m, Ar-H, 20H), δ 2.97 (s, 3H, (CH_3)).

Single crystal X-ray diffraction studies

X-ray diffraction data for $[PdCl_2(L)(PPh_3)]$ and $[PdCl_2(L)(AsPh_3)]$ were collected at 100K on a Bruker APEX II diffractometer using Mo-K_α radiation (λ = 0.71073 Å). Data collections were performed using a CCD area detector from a single crystal mounted on a glass fibre. Absorption corrections were based on equivalent reflections using SADABS [50]. The structures were solved using Superflip [51] and all of the structures were refined against F^2 in SHELXL [52] using Olex2 [53]. All of the non-hydrogen atoms were refined anisotropically. While all of the hydrogen atoms were located geometrically and refined using a riding model except for the hydrogen atoms that are attached to the amine N which were located in the difference map, in the case of $[PdCl_2(L)(PPh_3)]$ restraints were applied to the N-H distance and thermal parameters. Crystal structure and refinement data are given in Table 1. Crystallographic data for compounds $[PdCl_2(L)(PPh_3)]$ and $[PdCl_2(L)(AsPh_3)]$ have been deposited with the Cambridge

Crystallographic Data Centre(1498615, 1498616). Copies of the data can be obtained free of charge on application to CCDC, 12 Union Road, Cambridge CB2 1EZ, UK [fax(+44) 1223 336033, e-mail: deposit@ccdc.cam.ac.uk].

References

[1] E. Wong, C.M. Giandomenico, Chem. Rev.99 (1999) 2451.

[2] T.G. Drummond, M.G. Hill, J.K. Barton, Nat. Biotechnol. 21 (2003) 1192.

[3] E. Meggers, Angew. Chem. Int. Ed. 50 (2011) 2442.

[4] C.G. Hartinger, N. Metzler-Nolte, P.J. Dyson, Organometallics31 (2012) 5677.

[5] N.P. Barry, P.J. Sadler, Chem. Commun. 49 (2013) 5106.

[6] S. Ray, R. Mohan, J.K. Singh, M.K. Samantaray,M.M. Shaikh, D. Panda, P. Ghosh, J. Am. Chem. Soc.129 (2007) 15042.

[7] J. Ruiz, N.Cutillas, C. Vicente, M.D. Villa, G.Lopez, Inorg. Chem.44 (2005) 7365.

[8] E.J. Gao,C.Liu, M. C.Zhu, H.K. Lin,Q.Wu,L.Liu, Anti- Cancer Agents Med. Chem.9 (2009) 356.

[9] H.Daghriri, F.Huq, P.Beale, Coord. Chem. Rev.248 (2004) 119.

[10] E.Gao, C. Liu, M. Zhu, H. Lin, Q. Wu, L. Liu, Anti-Cancer Agents Med. Chem. 9 (2009) 356.

[11] A.S. Abu-Surrah, M. Kettunen, Curr. Med. Chem.13 (2006) 1337.

[12] A.C.F. Caires, Anti-Cancer Agents Med. Chem.7 (2007) 484.

[13] A.S. Abu-Surrah, H.H. Al-Sadoni, M.Y. Abdalla, Cancer Ther.6 (2008) 1.

[14] P. Souza, A.I. Matesanz, In Palladium: Compounds, Production and Applications; K.M. Brady, Ed. Nova Science Publishers: New York, (2011).

[15] A.I. Matesanz, C. Hernandez, A. Rodríguez, P.J. Souza, Inorg. Biochem. 105 (2011) 1613.

[16] B.R. Short, M.A. Vargas, J.C Thomas, S.O. Hanlon, M.C. Enright, In vitro activity of a novel compound, the metal ion chelating agent AQ+, against clinical isolates of Staphylococcus aureus. J. Antimicrob. Chemother. 57 (2006) 104.

[17] S.G. Sipka, C.R. kowol, S.M. Valiahdi, R. Eichinger, M.A. Jakupec, A. Roller. S. Shova, V.B. Arion, B.K. Keppler, Eur. J. Inorg. Chem. (2007) 2870.

[18] H. Zhang, R. Thomas, D. Oupicky, F. Peng, J. Biol. Inorg. Chem. 13 (2008) 47.

[19] J. DeRuiter, A.N. Brubaker, W.L. Whitmer, J.L. Stein, J. Med. Chem. 29 (1986)

2024.

[20] P. Hewawasam, W. Fan, J. Knipe, S.L. Moon, C.G. Boissard, V.K. Gribkoff,J.E. Starett, Bioorg. Med. Chem. Lett. 12 (2002) 1779.

[21] J. Rousell, E.B. Haddad, J.C. Mak, B.L. Webb, M.A. Giembycz, P.J. Barnes, Mol. Pharmacol. 49 (1996) 629.

[22] I.V. Ukrainets, V.O. Gorokhova, A.P. Benzuglyi, V.L. Sidorenko, Farm. Zh. 1 (2002) 75.

[23] T.J. Egan, D.C. Ross, P.A. Adams, FEBS Lett.352 (1994) 54.

[24] H. Daghriri, F. Huq, P. Beale, Coord. Chem. Rev. 248 (2004) 119.

[25] E. Gao, C. Liu, M. Zhu, H. Lin, Q. Wu, L. Liu, Anti-Cancer Agents Med. Chem. 9 (2009) 356.

[26] J. Chen, Y.W. Huang, G. Liu, Z. Afrasiabi, E. Sinn, S. Padhye, Y. Ma, Toxicol. Appl. Pharmacol. 197 (2004) 40.

[27] J. Marmur, J. mol. Biol. 3 (1961) 208.

[28] (a) E.C. Long, J.K. Barton, Acc. Chem. Res. 23 (1990) 271; (b) R.F. Pasternack, E.J. Gibbs, J.J. Villafranca, Biochemistry 22 (1983) 251.

[29] W.D. Wilson, L. Ratmeyer, M. Zhao, L. Strekowski, D. Boykin, Biochemistry 32 (1993) 4098.

[30] G. Zhao, H. Lin, S. Zhu, H. Sun, Y. Chen, J. Inorg. Biochem. 70 (1998) 219.

[31] Z.C. Liu, B.D. Wang, Z.Y. Yang, Y. Li, D.D. Qin, T. R. Li, Eur. J. Med. Chem. 44 (2009) 4477.

[32] E. Ramachandran, P. Kalaivani, R. Prabhakaran, M. Zeller, J.H. Barlett, P.O. Adero, T.R. Wagner, K. Natarajan, Inorg. Chim. Acta 385 (2012) 94.

[33] M.J. Hawkins, P. Soon-Shiong, N. Desaia, Adv. Drug Delivery Rev. 60 (2008) 876.

[34] C. Andre, Y.C. Guillaume, J. Chromatogr, B:Anal. Technol. Biomed. Life Sci. 801 (2004) 221.

[35] Y. Wang, H. Zhang, G. Zhang, W. Tao, S. Tang, J. Lumin. 126 (2007) 211.

[36] Z.C. Liu, B.D. Wang, Z.Y. Yang, Y. Li, D.D. Qin, T.R. Li, Eur. J. Med. Chem. 44 (2009) 4477.

[37] M. Bhattacharyya, U. Chaudhuri, R.K. Poddar, Biochem. Biophys. Res. Commun. 167 (1990) 1146.

[38] (a) E. Ramachandran, D. Senthil Raja, N. P. Rath, K. NatarajanInorg. Chem. 52 (2013) 1504. (b) T. Thirunavukkarasu, H. Puschmann, H.A. Sparkes, K. Natarajan, V.G. Gnanasounda, Appl. Organometal. Chem. (2017), http://dx.doi.org/10.1002/aoc.4111; (c) T. Thirunavukkarasu, H.A. Sparkes, K. Natarajan, V.G. Gnanasoundari, Inorg. Chim. Acta 473 (2018), 255; (d) T. Thirunavukkarasu, H. A. Sparkes, C. Balachandran, S. Awale, K. Natarajan, V.G. Gnanasoundari, J. Photochem & Photobiol, B: Biology 181 (2018), 59.

[39] G.Z. Chen, X.Z. Huang, J.G. Xu, Z.B. Wang, Z.Z. Zhang, Method of Fluorescent analysis, second ed., Science press, Beijing (1990).

[40] (a) J.N. Miller, Proc. Anal. Div. Chem. Soc. 16 (1979) 203; (b) K. Karami, Z. MehriLighvan, S.A. Barzani, A.Y. Faal, M. Poshteh-Shirani, T. Khayamian, V. Eignerc, M. Dusekc, NewJ.Chem.39 (2015) 8708; (c) F.A. Beckford, M. Shaloski, G. Leblanc, J. Thessing, L.C.L. Alleyne, A.A. Holder, L. Li, N.P. Seeram, Dalton Trans. (2009) 10757.

[41] A.I. Vogel, Text Book of Practical Organic Chemistry, 5th Ed. Longman. London (1989)

[42] (a) S. Purohit, A.P. Koley, L.S. Prasad, P.T. Manoharan, S. Ghosh, Inorg. Chem. 28 (1989) 3735; (b) J.L. Burmeister, F. Basolo, Inorg.Chem. 3 (1964) 1587.

[43] S. Purohit, A.P. Koley, L.S. Prasad, P.T. Manoharan, S. Ghosh, Inorg. Chem. 28(1989) 3735.

[44] J.L. Burmeister, F. Basolo, Inorg. Chem. 3 (1964) 1587.

[45] D. Senthil Raja, N.S.P. Bhuvanesh, K. Natarajan, Inorg. Chem. (50) 2011 12852.

[46] J. Marmur, J. mol. Biol. 3 (1961) 208.

[47] Pique E.M, Huey R (2010). The Autodock 4.2 molecular graphics system. http://autodock.scripps.edu/downloads/autodock-registration/autodock-4-2-download-page.

[48] K.A. Majorek, P.J. Porebski, A. Dayal, M.D. Zimmerman, K. Jablonska, A.J. Stewart, M .Chruszca, W. Minor. Structural and immunologic characterization of bovine, horse and rabbit serum albumins. Mol. Immunol. 52 (2012) 174.

[49] (a) L. Palatinus, G. Chapuis,. J. Appl. Cryst., 40 (2007) 786; (b) L. Palatinus, A. Vander Lee, J. Appl. Cryst. 41 (2008) 975; (b) L. Palatinus, S.J. Prathapa, S. Van Smaalen, J. Appl. Cryst. 45 (2012) 575.

[50] M. Blagosklonny, W.S. EI-diery, Int. J. Cancer67 (1996) 386.

[51] G.M. Sheldrick, SADABS V2014/4, University of Gottingen, Germany.

[52] G.M. Sheldrick, ActaCryst. A 64 (2008) 112.

[53] O.V. Dolomanov, L.J. Bourhis, R.J. Gildea, J.A.K. Howard, H. Puschmann, OLEX2: a complete structure solution, refinement and analysis program. J. Appl. Cryst. 42 (2009) 339.